Ceramics-Silikáty 61 (3), 209-213 (2017)
www.ceramics-silikaty.cz doi: 10.13168/cs.2017.0018

MICROSTRUCTURE, PHASE EVOLUTION AND MICROWAVE DIELECTRIC PROPERTIES OF Li_2O AND Ga_2O_3 DOPED ZINC ORTHOSILICATE

SHIN KIM*, SANG-OK YOON**, YUN-HAN KIM**, SEONG-MIN JEONG***, #HOON PARK****

*Hasla Co., Ltd, Gangneung 25452, Korea
**Department of Materials Engineering, Graduate School, Gangneung-Wonju National University, Gangneung 25457, Korea
***Energy & Environmental Division, Korea Institute of Ceramic Engineering and Technology(KICET), Jinju 52851, Korea
****Department of Advanced Materials Engineering, Korea Polytechnic University, Siheung 15073, Korea

#E-mail: ph8236@kpu.ac.kr

Submitted February 15, 2017; accepted April 10, 2017

Keywords: Zinc orthosilicate, Li_2O, Ga_2O_3, Liquid phase sintering, Dielectric constant, Quality factor

Microstructure, phase evolution, and microwave dielectric properties of Li_2O and Ga_2O_3 doped zinc orthosilicate having the composition of $Zn_{1.9}Si_{1.05}O_4$, i.e. the $Zn_{1.9-2x}Li_xGa_xSi_{1.05}O_4$ system where x = 0.02 ~ 0.10, were investigated. $LiGaSiO_4$ and $ZnGa_2O_4$ are observed as the secondary phase. The densification occurred by the liquid phase in the all specimens. The densification curves showed a sigmoidal shape. As the amount of Li_2O and Ga_2O_3 increased, the temperature indicating the maximum value of bulk density in each composition decreased from 1250°C to 1100°C. The value of dielectric constant against the sintering temperature showed a similar tendency as that of the bulk density. The presence of the liquid phase and the insufficient grain growth may cause the deterioration of the quality factor. The dielectric constant and the quality factor of the specimen of x = 0.08 sintered at 1100°C were 6.28 and 27.097 GHz, respectively.

INTRODUCTION

Microwave and millimeter-wave dielectric ceramics have been developed for a wide range of applications in telecommunication, such as cellular phone, wireless LAN, global position satellite (GPS), military radar system, intelligent transport system (ITS), and direct broadcast satellite [1, 2]. Dielectric ceramics with low loss can be classified into three categories according to their applications. One of them with low dielectric constant and high Q is for millimeter-wave and substrate applications [2]. For these applications, silicates are proposed to be good candidates because of their low dielectric constant [2]. Zinc orthosilicate (Zn_2SiO_4) ceramics which is the only stable compound at atmospheric pressure in the ZnO–SiO_2 binary system [3, 4] having the willemite structure showed excellent millimeter-wave dielectric properties when the sintering were carried out from 1280 to 1340°C; the dielectric constant value of 6.6 and the quality factor (Q × f) value of 219.000 GHz [5].

To apply zinc orthosilicate as the material for low temperature co-fired ceramics (LTCC) with the electrodes such as Ag or Cu, on the other hand, many efforts have been made to reduce the sintering temperature below 900 ~ 950°C. As shown in Table 1, the addition of various sintering aids allows to lower the sintering temperature of zinc orthosilicate based ceramics [6-18]. According to Table 1, B_2O_3 including H_3BO_3 was well used as the sintering aids and was effective to reduce the sintering temperature, however, it was reported that the addition of B_2O_3 on the aqueous slurry for the tape-casting process which is generally to be applied on the LTCC manufacturing process increased the viscosity of the slurry significantly and decreased the tensile strength of the green tapes as well as the density due to lower dispersion of particle [19]. Therefore, it needs to pay attention to apply of B_2O_3 on the aqueous slurry. In this work, to investigate the possibility of using Li_2O and Ga_2O_3 doped zinc orthosilicate for low temperature co-fired ceramic substrate materials, microstructure, phase evolution, and microwave dielectric properties of $Zn_{1.9}Si_{1.05}O_4$ which was doped with Li_2O and Ga_2O_3 are investigated.

EXPERIMENTAL

Li_2O and Ga_2O_3 doped zinc orthosilicate ceramics were prepared by a conventional solid-state reaction. ZnO, SiO_2 with a quartz form, Li_2CO_3, and Ga_2O_3 were used as starting powders. All of the powders with the purity of 3N were manufactured by High Purity Chemicals Co. Ltd, Japan. The proper ratio of starting powders in the $Zn_{1.9-2x}Li_xGa_xSi_{1.05}O_4$ system where x = 0.02 ~ 0.10 was ball-milled using zirconia balls and

ethanol as the medium in a polyethylene container for 12 h. After the drying process, powder mixtures were calcined at 900°C for 10 h using an alumina crucible. The disk-type specimens were obtained by a sintering process between 1000°C and 1250°C for 2 h after a uniaxial pressing at 50 MPa. The microstructure of the sintered specimen was characterized by a field emission scanning electron microscope (FE-SEM, S-4200, Hitachi, Japan) after a thermal etching. The crystalline phases of the sintered specimen were identified by a powder X-ray diffractometer (D/MAX-2500V/PC, Rigaku, Japan) using pulverized powder. The bulk density of the sintered specimens was measured by the Archimedes method. The microwave dielectric properties of the disk-type specimens were measured by a network analyzer (HP8720ES, Agilent, USA) using a Hakki-Coleman fixture configuration.

RESULTS AND DISCUSSION

The sintering of zinc orthosilicate has been reported to be carried out at 1300 ~ 1350°C and the densification of it proceeded with the presence of the liquid phase [20, 21]. Nguyen et al. reported that the densification and grain growth of Zn deficient zinc orthosilicate sintered at 1300°C occurred by the formation of a Si-rich liquid phase [21]. Yoon et al. also pointed out that the liquid phase enhanced the sinterability of $Zn_{2-2x}Si_{1+x}O_4$ ceramics sintered at 1350°C [20]. The typical microstructures of Li_2O and Ga_2O_3 doped zinc orthosilicate are shown in Figure 1; for the specimen of x = 0.02 sintered at 1250°C (Figure 1a) and that of x = 0.06 sintered at 1150°C (Figure 1b). The photographs show a dense microstructure. As shown in Figure 1a, the flat-faced grains are observed, implying that the grain growth occurs

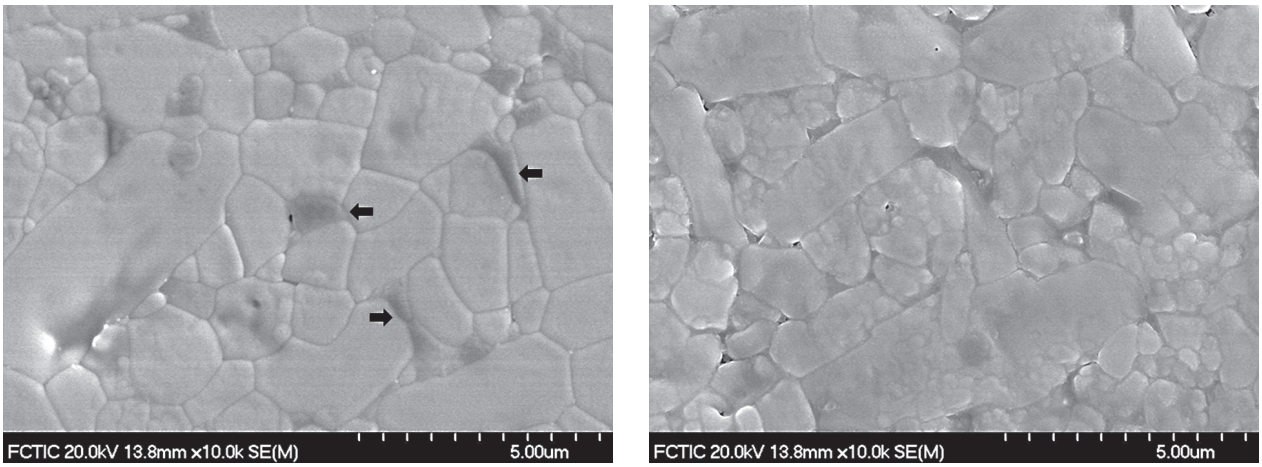

a) b)

Figure 1. FE-SEM photographs of $Zn_{1.9-2x}Li_xGa_xSi_{1.05}O_4$; a) x = 0.02 sintered at 1250°C and b) 0.06 sintered at 1150°C.

Table 1. The summarized sintering aids and their content for zinc orthosilicate based ceramics.

compound	content of sintering aid	sintering temperature (°C)	reference number
Zn_2SiO_4	0.2 wt. % Li_2CO_3	1050	6
ZnO–0.6 SiO_2	5 wt. % Li_2CO_3 – 4 wt. % Bi_2O_3	910	7
$Zn_{1.8}SiO_{3.8}$	20 mol. % B_2O_3	900	8
	12 mol. % V_2O_5	875	9
	8 mol. % Bi_2O_3	885	10
	25 mol. % B_2O_3	900	11
Zn_2SiO_4	10 - 20 wt. % BaO–B_2O_3	900	12
	20 wt. % ZnO–B_2O_3–SiO_2 glass	900	13
$(Zn_{0.8}Mg_{0.2})_2SiO_4$–$TiO_2$	3 wt. % Li_2O–B_2O_3–SiO_2 glass	870	14
	3 wt. % Li_2O–B_2O_3	900	15
	3 wt. % CaO–B_2O_3–SiO_2 glass	950	16
Zn_2SiO_4–$CaTiO_3$	4 wt. % Li_2CO_3–H_3BO_3	950	17
$Zn_{1.87}SiO_{3.87}$–$Ba_3(VO_4)_2$	3 wt. % B_2O_3	925	18

through the solution-reprecipitation process of the liquid phase sintering. According to the theory of liquid phase sintering, the dissolved solid diffused through the liquid and precipitated onto solid surfaces with lower energy during the solution-reprecipitation process [22, 23]. And this process allowed to form the larger grains grown by the expense of the smaller grains and the growing large grains are flat faced. Although the photograph for the specimen of x = 0.06 shows a dense microstructure, the grain size is dispersed, suggesting that the grain growth is going on after the rearrangement process.

For the specimen of x = 0.02, on the other hand, the dark-colored grains marked by arrows are observed. In the SE mode of FE-SEM, it is indicated that the grains with dark color are composed of lighter elements; the observed dark-colored grains may contain at least Li^+ ion which is lightest element in this work. As shown in the powder X-ray diffraction patterns of Li_2O and Ga_2O_3 doped zinc orthosilicate (Figure 2), $LiGaSiO_4$ with an ordered, phenakite-derivative rhombohedral structure (space group: R3, ICDD file number: 79-0211) marked by a closed diamond are detected in the compositions of x = 0.08 and 0.10. From these results, it is considered that the dark-colored grains may be a liquid composed of Li_2O–Ga_2O_3–SiO_2 at the sintering temperature. It is reported that the glass forming region existed in the Li_2O–Ga_2O_3–SiO_2 ternary system supports this suggestion [24]. $LiGaSiO_4$ may be precipitated from the liquid during the cooling process after the sintering.

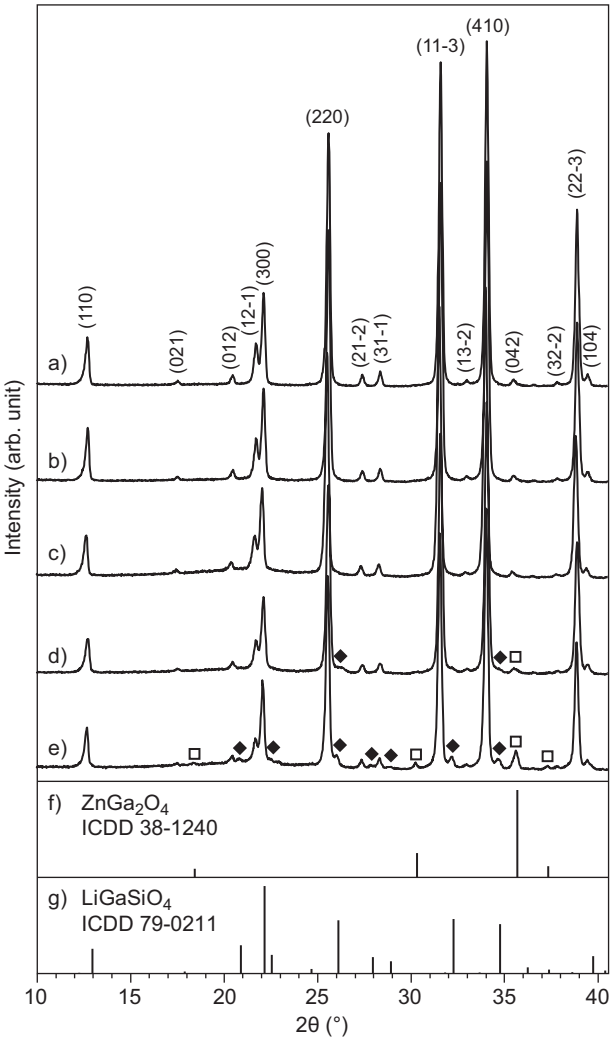

Figure 2. Powder X-ray diffraction patterns of $Zn_{1.9-2x}Li_xGa_xSi_{1.05}O_4$; a) x = 0.02, b) 0.04, c) 0.06, d) 0.08, e) 0.10, f) $ZnGa_2O_4$ (ICDD File 38-1240), and g) $LiGaSiO_4$ (ICDD File 79-0211).

Additional diffraction peaks marked by an open square correspond with $ZnGa_2O_4$ (space group: Fm3m, ICDD file number: 38-1240) having a cubic spinel structure are shown in Figure 2. It is reasonable that $ZnGa_2O_4$ is assumed to form in the Li_2O–ZnO–Ga_2O_3––SiO_2 quaternary system because of the $ZnGa_2O_4$ having $A^{2+}B_2^{3+}O_4$ general formula of the normal spinel (A = Zn, B = Ga). On the other hand, judging from the $Li_{0.5(1-x)}Zn_xFe_{2.5-0.5x}O_4$ solid solution (or $Li_yZn_{1-2y}Fe_{2+y}O_4$ where y = 1 - 2x, i.e., two Zn^{2+} sites of $ZnFe_2O_4$ are substituted by Li^+ and Fe^{3+} ions) with the spinel structure (space group: , ICDD file number: 71-1262~71-1270) implies that the spinel which is composed of Li_2O–ZnO–Ga_2O_3 might exist because of the similarity of the ionic radius for Fe^{3+} (0.0645 nm, coordination number = 6) and Ga^{3+} (0.0620 nm) [25]. Indeed, there was a research for the solid solution between $ZnGa_2O_4$ with the normal spinel and $Li_{0.5}Ga_{2.5}O_4$ with the inverse one within the whole range [26]. However, the lattice parameter of $Li_{0.5}Ga_{2.5}O_4$ was reported as between 8.203 and 8.210 Å which are smaller than that of $ZnGa_2O_4$ (a_0 = 8.3349 Å) [27]. Therefore, from the result that the diffracted peaks of the spinel structure observed at slightly lower angle than those of $ZnGa_2O_4$ as shown in Figure 2e and f, the formed spinel may be considered to $ZnGa_2O_4$ solid solution rather than that of $Li_{0.5}Ga_{2.5}O_4$.

From the results that the obvious shift of diffracted peaks for zinc orthosilicate does not occur and the secondary phases such as $LiGaSiO_4$ and $ZnGa_2O_4$ are observed, the introduction of Li^+ and Ga^{3+} ions on zinc orthosilicate may be negligible. The origin of the formation for $ZnGa_2O_4$ is unclear; the precipitation from the liquid or the solid state reaction between ZnO and Ga_2O_3. In any case, it is interesting that the secondary phase of β-spodumene solid solution having a composition close to $LiAlSi_3O_8$ was formed in the Li_2O and Al_2O_3 doped zinc orthosilicate system [28] whereas $LiGaSiO_4$ and $ZnGa_2O_4$ are formed in this work. Further study about the formation of the secondary phases in these systems is necessary. Besides $LiGaSiO_4$ and $ZnGa_2O_4$, other secondary phases such as ZnO or SiO_2, which were respectively reported as the secondary phases formed in the stoichiometric composition of zinc orthosilicate or SiO_2-rich one, are not observed [21].

Bulk density of Li_2O and Ga_2O_3 doped zinc orthosilicate, i.e., $Zn_{1.9-2x}Li_xGa_xSi_{1.05}$, x = 0.02 ~ 0.10, as a function of the sintering temperature is shown in Figure 3. All of the densification curves show a sigmoidal

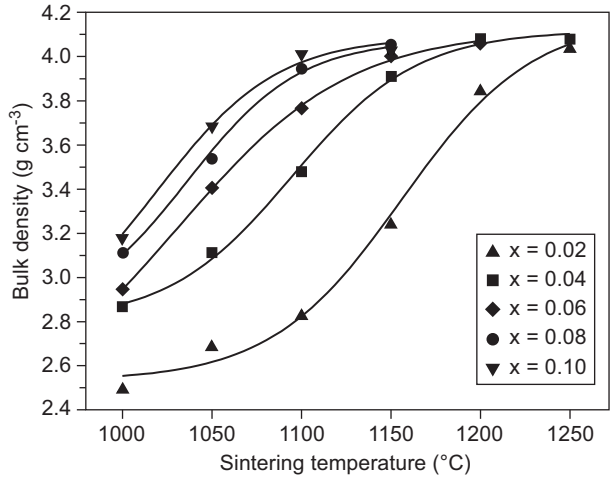

Figure 3. Bulk density of $Zn_{1.9-2x}Li_xGa_xSi_{1.05}O_4$ as a function of the sintering temperature.

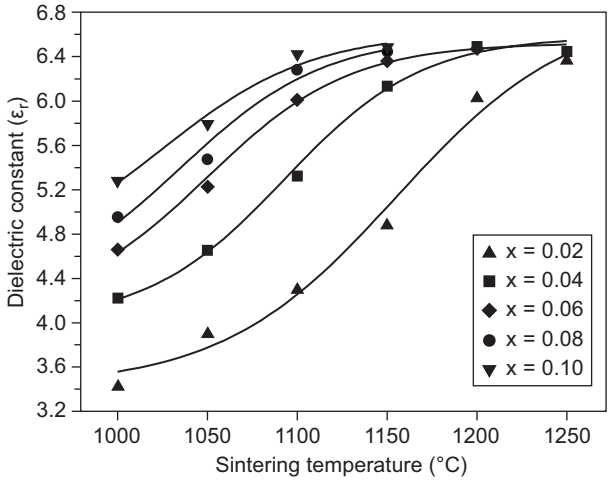

Figure 4. Dielectric constant of $Zn_{1.9-2x}Li_xGa_xSi_{1.05}O_4$ as a function of the sintering temperature.

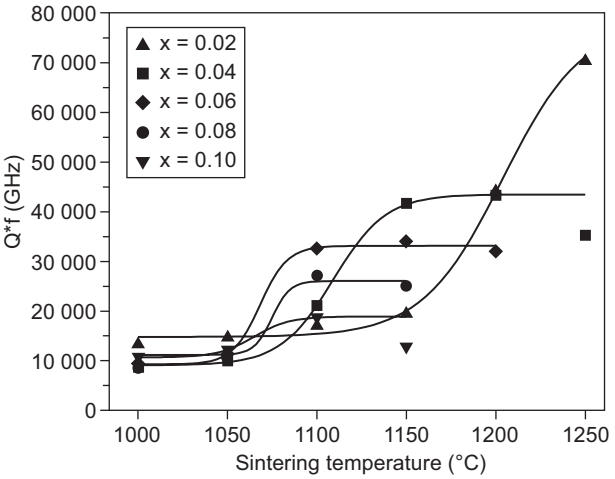

Figure 5. Quality factor of $Zn_{1.9-2x}Li_xGa_xSi_{1.05}O_4$ as a function of the sintering temperature.

shape. As the amount of Li_2O and Ga_2O_3 increases, the temperature indicating the maximum value of bulk density in each composition decreases from 1250°C to 1100°C, implying that densification is influenced by the amount of the liquid. The value of dielectric constant against the sintering temperature shows a similar tendency as that of the bulk density as shown in Figure 4. The quality factor of Li_2O and Ga_2O_3 doped zinc orthosilicate versus the sintering temperature is shown in Figure 5. The value of the quality factor deceases as the amount of Li_2O and Ga_2O_3 increases. The presence of the liquid phase and the insufficient grain growth as shown in Figure 1b may cause the deterioration of the quality factor. The quality factor, i.e., the inverse of the dielectric loss, is associated with imperfection in the crystal structure, e.g., impurities, microstructural defects, grain boundaries, porosity, microcracks, and random crystallite orientation [29, 30]. The dielectric constant and the quality factor of the specimen of x = 0.08 sintered at 1100°C are 6.28, and 27,097 GHz, respectively.

CONCLUSION

Microstructure, phase evolution, and microwave dielectric properties of Li_2O and Ga_2O_3 doped zinc orthosilicate having the composition of $Zn_{1.9}Si_{1.05}O_4$, i.e. the $Zn_{1.9-2x}Li_xGa_xSi_{1.05}O_4$ system where x = 0.02 ~ 0.10, were investigated. $LiGaSiO_4$ and $ZnGa_2O_4$ are observed as the secondary phase. The densification occurred by the liquid phase sintering in the all specimens. The densification curves showed a sigmoidal shape. As the amount of Li_2O and Ga_2O_3 increased, the temperature indicating the maximum value of bulk density in each composition decreased from 1250°C to 1100°C, implying that doped Li_2O and Ga_2O_3 participate in the formation of the liquid and bulk density is influenced by the amount of the liquid. The value of dielectric constant against the sintering temperature showed a similar tendency as that of the bulk density. The value of the quality factor deceased as the amount of Li_2O and Ga_2O_3 increased. The presence of the liquid phase and the insufficient grain growth may cause the deterioration of the quality factor. The dielectric constant and the quality factor of the specimen of x = 0.08 sintered at 1100°C were 6.28, and 27,097 GHz, respectively.

REFERENCES

1. Narang S. B., Bahel S. (2010): Low loss dielectric ceramics for microwave applications: a review. *Journal of Ceramic Processing Research*, *11*(3), 316-321.
2. Ohsato H. (2005): Research and development of microwave dielectric ceramics for wireless communications. *Journal of the Ceramic Society of Japan*, *113*(11), 703-711. doi:10.2109/jcersj.113.703

3. Takesue M., Hayashi H., Smith R. L. (2009): Thermal and chemical methods for producing zinc silicate (willemite): A review. *Progress in Crystal Growth and Characterization of Materials*, *55*(3-4),98-124. doi:10.1016/j.pcrysgrow.2009.09.001
4. Eldem M. A., Orton B. R., Whitaker A. (1987): Phase equilibria in the system ZnO-B_2O_3-SiO_2 at 950° C. *Journal of Materials Science*, *22*(11), 4139-4143. doi:10.1007/BF01133370
5. Guo Y., Ohsato H., Kakimoto K.-I. (2006): Characterization and dielectric behavior of willemite and TiO_2-doped willemite ceramics at millimeter-wave frequency. *Journal of the European Ceramic Society*, *26*(10-11), 1827-1830. doi:10.1016/j.jeurceramsoc.2005.09.008
6. Valant M., Suvorov D., Pullar R. C., Sarma K., Alford N. M. (2006): A mechanism for low-temperature sintering. *Journal of the European Ceramic Society*, *26*(13), 2777-2783. doi:10.1016/j.jeurceramsoc.2005.06.026
7. Zou J.-L., Zhang Q.-L., Yang H., Sun H.-P. (2006): A New System of Low Temperature Sintering ZnO–SiO_2 Dielectric Ceramics. *Japanese Journal of Applied Physics*, *45*(5A), 4143-4145. doi:10.1143/JJAP.45.4143
8. Kim J.-S., Nguyen N.-H., Lim J.-B., Paik D.-S., Nahm S., Paik J.-H., Kim J.-H., Lee H.-J. (2008): Low-Temperature Sintering and Microwave Dielectric Properties of the Zn_2SiO_4 Ceramics. *Journal of the American Ceramic Society*, *91*(2), 671–674. doi:10.1111/j.1551-2916.2007.02187.x
9. Kim J.-S., Song M.-E., Joung M.-R., Choi J.-H., Nahm S., Paik J.-H., Choi B.-H., Lee H.-J. (2008): Low-Temperature Sintering and Microwave Dielectric Properties of V_2O_5-Added Zn_2SiO_4 Ceramics. *Journal of the American Ceramic Society*, *91*(12), 4133-4136. doi:10.1111/j.1551-2916.2008.02785.x
10. Kim J.-S., Nguyen N.-H., Song M.-E., Lim J.-B., Paik D.-S., Nahm S., Paik J.-H., Choi B.-H., Yu S.-J. (2009): Effect of Bi_2O_3 Addition on the Sintering Temperature and Microwave Dielectric Properties of Zn_2SiO_4 Ceramics. *International Journal of Applied Ceramic Technology*, *6*(5), 581-586. doi:10.1111/j.1744-7402.2008.02335.x
11. Kim J.-S., Song M.-E., Joung M.-R., Choi J.-H., Nahm S., Gu S.-I., Paik J.-H., Choi B.-H. (2010): Effect of B_2O_3 addition on the sintering temperature and microwave dielectric properties of Zn_2SiO_4 ceramics. *Journal of the European Ceramic Society*, *30*(2), 375-379. doi:10.1016/j.jeurceramsoc.2009.04.028
12. Chen S., Zhang S., Zhou X., Lv X., Li Y. (2011): Low temperature preparation of the Zn_2SiO_4 ceramics with the addition of BaO and B_2O_3. *Journal of Materials Science: Materials in Electronics*, *22*(9), 1274-1281. doi:10.1007/s10854-011-0299-8
13. Tang K., Wu Q., Xiang X. (2012): Low temperature sintering and microwave dielectric properties of zinc silicate ceramics. *Journal of Materials Science: Materials in Electronics*, *23*(5), 1099-1102. doi:10.1007/s10854-011-0555-y
14. Zhang Q. L., Yang H., Zou J. L. (2008): Low-temperature sintering of $(Zn_{0.8}\ Mg_{0.2})_2SiO_4$–$TiO_2$ ceramics. *Materials Letters*, *62*(23), 3872-3874. doi:10.1016/j.matlet.2008.05.008
15. Zhang Q. L., Yang H., Zou J. L. (2009): Microwave dielectric properties and low-temperature sintering of $(Zn_{0.8}Mg_{0.2})_2SiO_4$–$TiO_2$ ceramics with Li_2O–B_2O_3. *Journal of Materials Science: Materials in Electronics*, *20*(2), 181-185. doi:10.1007/s10854-008-9688-z
16. Li B., Tang B., Zhang S., Jiang H. (2011): Low-temperature sintered $(ZnMg)_2SiO_4$ microwave ceramics with TiO_2 addition and calcium borosilicate glass. *Ceramics-Silikáty*, *55*(1), 14-19.
17. Dou G., Zhou D., Guo M., Gong S., Hu, Y. (2012): Low-temperature sintered Zn_2SiO_4–$CaTiO_3$ ceramics with near-zero temperature coefficient of resonant frequency. *Journal of Alloys and Compounds*, *513*, 466-473. doi:10.1016/j.jallcom.2011.10.089
18. Lv Y., Zuo R. (2013). (2013): Effect of the B_2O_3 addition on the sintering behavior and microwave dielectric properties of $Ba_3(VO_4)_2$–$Zn_{1.87}SiO_{3.87}$ composite ceramics. *Ceramics International*, *39*(3), 2545-2550. doi:10.1016/j.ceramint.2012.09.014
19. Li S., Zhang Q., Yang H. (2013): Effect of B_2O_3 on the aqueous tape casting and microwave properties of Li_2O–Nb_2O_5–TiO_2 ceramics. *Progress in Natural Science: Materials International*, *23*(2), 152-156. doi:10.1016/j.pnsc.2013.02.007
20. Yoon S.-O., Kim Y.-H., Jeong S.-M., Kim S.-J., Jo S.-R., Kim S. (2015): Sintering and Microwave Dielectric Properties of $Zn_{2-2x}Si_{1+x}O_4$ Ceramics. *Journal of the Korean Institute of Electrical and Electronic Material Engineers*, *28*(7), 428-432. doi:10.4313/JKEM.2015.28.7.428
21. Nguyen N.-H., Lim J.-B., Nahm S., Paik J.-H., Kim J.-H. (2007): Effect of Zn/Si Ratio on the Microstructural and Microwave Dielectric Properties of Zn_2SiO_4 Ceramics. *Journal of the American Ceramic Society*, *90*(10), 3127-3130. doi:10.1111/j.1551-2916.2007.01891.x
22. German R. M. (1985). Liquid Phase Sintering. Plenum Press.
23. German R. M., Suri P., Park S. J. (2009): Review: liquid phase sintering. *Journal of Materials Science*, *44*(1), 1-39. doi:10.1007/s10853-008-3008-0
24. Suzuki T., Arai Y., Ohishi Y. (2007): Crystallization processes of Li_2O–Ga_2O_3–SiO_2–NiO system glasses. *Journal of Non-Crystalline Solids*, *353*(1), 36-43. doi:10.1016/j.jnoncrysol.2006.09.032
25. Shanon R. D. (1976): Revised effective ionic radii and systematic studies of interatomic distances in halides and chalcogenides. *Acta Crystallographica Section A*, *32*, 751-767. doi:10.1107/S0567739476001551
26. Park K. H., Park H. L., Mho S. I. (2001): Compositional dependence of photoluminescence (PL) of $ZnGa_2O_4$: Li^+; Li^+ ion incorporated as $LiGa_5O_8$, $LiGaO_2$, and Li_2O. *Journal of Luminescence*, *93*(3), 205–212. doi:10.1016/S0022-2313(01)00198-3
27. Hirano M., Imai M., Inagaki M. (2000): Preparation of $ZnGa_2O_4$ Spinel Fine Particles by the Hydrothermal Method. *Journal of the American Ceramic Society*, *83*(4), 977-979. doi:10.1111/j.1151-2916.2000.tb01310.x
28. Kim Y. H., Kim S., Jeong S. M., Kim S. J., Yoon S. O. (2015): Phase Evolution, Microstructure and Microwave Dielectric Properties of $Zn_{1.9-2x}Li_xAl_xSi_{1.05}O_4$ Ceramics. *Journal of the Korean Ceramic Society*, *52*(3), 215-220. doi:10.4191/kcers.2015.52.3.215
29. Gurevich V. L., Tagantsev A. K. (1991): Intrinsic dielectric loss in crystals. *Advances in Physics*, *40*(6), 719-767. doi:10.1080/00018739100101552
30. Alford N. M., Penn S. J. (1996): Sintered alumina with low dielectric loss. *Journal of Applied Physics*, *80*(10), 5895-5898. doi:10.1063/1.363584